

Supplemental information

Seawater pH reconstruction using boron isotopes in multiple planktonic foraminifera species with different depth habitats and their potential to constrain pH and pCO₂ gradients

Maxence Guillermic^{1,6}, Sambuddha Misra^{2,3}, Robert Eagle^{1,5}, Alexandra Villa⁶, Fengming Chang⁴, Aradhna Tripathi^{1,5,6}

¹ Laboratoire Géosciences Océan UMR6538, UBO, Institut Universitaire Européen de la Mer, Rue Dumont d'Urville, 29280, Plouzané, France

² The Godwin Laboratory for Palaeoclimate Research, Department of Earth Sciences, University of Cambridge, UK

³ Indian Institute of Science, Centre for Earth Sciences, Bengaluru, Karnataka 560012, India

⁴ Key Laboratory of Marine Geology and Environment, Institute of Oceanology, Chinese Academy of Sciences, Qingdao 266071, China

⁵ Institute of the Environment and Sustainability, Department of Atmospheric and Oceanic Sciences, University of California – Los Angeles, CA 90095, USA

⁶ Department of Earth, Planetary, and Space Sciences, UCLA, University of California – Los Angeles, Los Angeles, CA 90095 USA

Supplemental Figures

Figure S1: An example of the impact of seasonality on results. Based on data from GLODAP used for site FC13-a. Seasonality has less of an impact than a change in the depth habitats.

Figure S2: Figure showing the offset $\Delta^{11}\text{B} = \delta^{11}\text{B}_{\text{carbonate}} - \delta^{11}\text{B}_{\text{borate}}$ versus calcification depth, red symbols are from Arabian Sea, green from Indian Ocean and blue from the WEP, blue with black line symbols are data from site A14. This figure highlights a decrease of $\delta^{11}\text{B}_{\text{carbonate}}$ for *T. sacculifer* and *G. ruber* with a deeper depth habitat.

Figure S3: Boron isotopic measurements of (A) SML shallow mixed-layer foraminifera, (B) deep-dweller foraminifera plot against the $\delta^{11}\text{B}_{\text{borate}}$. Grey lines represent the theoretical elevation or reduction of microenvironment pH (see main text for calculations). This figure permits to recalculate based on our $\delta^{11}\text{B}_{\text{carbonate}}$ the microenvironment pH of the species investigated.

Figure S4: Multi-panels figure showing the correlation between B/Ca and boron geochemistry and different variables. A to C show comparison of B/Ca and A) $[\text{B}(\text{OH})_4^-]/[\text{HCO}_3^-]$, B) $\delta^{11}\text{B}_{\text{carbonate}}$ and C) temperature. Panel D) shows the correlation between $\delta^{11}\text{B}_{\text{carbonate}}$ and temperature. Highlighted in yellow are mixed-layer dwelling species and in blue are deeper dwelling species. Symbol in brackets is high B/Ca; this point is included in the linear regressions.

Figure S5: Boron geochemistry against water depth. A) $\delta^{11}\text{B}_{\text{carbonate}}$ versus water depth, B) B/Ca against water depth and C) $\delta^{11}\text{B}_{\text{carbonate}}$ versus calcification depth and linear regressions for *G. ruber*, *T. sacculifer* (w/o sacc), *T. sacculifer* (sacc) and *O. universa*.

Figure S6: Percent difference between calculated pH and in-situ pH versus the offset applied. For a % of 0 the calculated pH is equal to the in-situ pH. The corrected values in Fig. 8 and 9 are calculated using an offset of 0.20‰ and 0.75‰ for *G. ruber* and *T. sacculifer* (w/o sacc) respectively.

Supplemental Tables

Table S1: Elemental ratios of multi-elemental standards utilized in this study.

Table S2: Reproducibility of boron isotope standards..

Table S3: Reproducibility of elemental ratios for CamWuellestorfi standard.

Table S4: Seasonality of foraminifera utilized in this study.

Table S5: Mg/Ca-T calibrations used for reconstructions and $\delta^{18}\text{O}_w$ -T calibrations used for calcification depth reconstructions.

Table S6: Calcification depth (CD) calculations from $\delta^{18}\text{O}$ (CD1), Mg/Ca (CD2) and literature (CD3).

Table S7: Pre-industrial in-situ parameters estimated using calcification depths for each species and calculated parameters based on analytical results.

Trace element standards

A series of multi-element standards (Table S1) with fixed Ca concentration and variable B, Mg, Sr, Mn, Ba, Zn, Cd, U, Li, Al and Fe concentrations were prepared for elemental ratios analysis in Brest following the method developed by Yu et al., (2005). Multi-element stock standard mixtures were prepared gravimetrically by spiking a 10,000 ppm Ca standard with appropriate amounts of Li, B, Al, Mn, Zn, Sr, Cd and U mono-elemental 1,000 ppm (SCP Science). They were diluted with OPTIMA grade HNO₃ acid and 18.2 MΩ.cm⁻¹ water to reach a 0.28M HNO₃ final solution. The stock standards (1500 ppm Ca) were prepared in 500mL cleaned PFA bottles. Working standards were made by diluting the stock solutions to a final concentration of 100 ppm Ca. The multi-element standards were calibrated at the University of Cambridge, elemental ratios are presented in Table S1. An external standard CamWuellestorfi (Misra et al., 2014a) was used in Brest for cross-calibration and reproducibility (Table S3).

Potential contaminations

Possible contamination of samples due to presence of silicate minerals was monitored with the Fe/Mg ratio. Samples with Fe/Mg > 0.1 mol/mol would be rejected due to potential contamination by silicate minerals (Barker et al., 2003). Samples (site E035 excluded) have an average Fe/Mg of 0.03 ± 0.05 mol/mol (2SD, n=42), meaning that silicate minerals have been efficiently removed during our cleaning.

Contribution of Mn-Fe-oxide coatings to Mg/Ca ratio has been calculated to be 0.5 μmol/mol Mg/Ca (change for 5 μmol/mol Mn/Ca ratio Barker et al., 2003). The maximum Mn/Ca ratio in our samples is 89 μmol/mol which can lead to a potential contribution of ~9 μmol/mol Mg/Ca or in other words a decrease of 0.1°C in our reconstructed temperatures. However, the calibration error is much larger and is estimated to be ~1.4°C (Dekens et al., 2002). The range in Mn/Ca values in our samples is 0.021 ± 0.033 mmol/mol (2SD, n=42) which allows us to not be ignore *Mn-Fe-oxide* coating related complications. Additionally, no correlations were found between Mg/Ca and Fe/Ca ($R^2=0.006$) or with Mn/Ca ($R^2=0.008$), and between B/Ca ratio and Mn/Ca ($R^2=0.003$) or Fe/Ca ($R^2=0.062$) ratios.

Contamination by clays was monitored with Ti/Ca calculated from blank corrected intensities. Al/Ca ratios were not reliable as we are using an alumina injector for HF matrix in our lab. A minor correlation was found between Ti/Ca and Mg/Ca ($R^2=0.1388$) but none with B/Ca ($R^2=0.0887$).

Calcification depth determination

The first approach involves comparing measured $\delta^{18}\text{O}_c$ with theoretical predictions of $\delta^{18}\text{O}_c$ based on vertical profiles of temperature and the $\delta^{18}\text{O}$ of seawater ($\delta^{18}\text{O}_w$). We assume $\delta^{18}\text{O}_c$ is in equilibrium with seawater. First, $\delta^{18}\text{O}_w$ was calculated using location-specific $\delta^{18}\text{O}_w$ -salinity relationships and salinity profiles. We used salinity values from the World Ocean Atlas database (Boyer et al., 2013). Oxygen isotopes may be affected by both temperature and salinity. As our sites present different hydrographic settings and freshwater inputs, location-specific $\delta^{18}\text{O}_w$ -salinity relationship relationships are utilized for accurate $\delta^{18}\text{O}_w$ reconstructions. For Site CD107-a, we used a $\delta^{18}\text{O}_w$ -salinity relationship of $0.56 \cdot S - 19.3$ (Duplessy et al., 1991). For FC01-a and FC02-a, we used a $\delta^{18}\text{O}_w$ -salinity relationship of $0.24 \cdot S - 7.8$ (Sime et al., 2005), and for FC13-a and FC12-b, we used a $\delta^{18}\text{O}_w$ -salinity relationship of $0.28 \cdot S - 9.24 - 0.27$ (Rosteket al., 1993). Then, we used the calculated ambient $\delta^{18}\text{O}_w$ in concert with: (1) temperature profiles from the World Ocean Atlas database (Boyer et al., 2013), and (2) published calcite-water oxygen isotope fractionation factors, to calculate theoretical values for $\delta^{18}\text{O}_c$. Species-

specific relationships were used when available, including for *T. sacculifer* (Mulitza et al., 2003), *G. ruber* (Mulitza et al., 2003), and *O. universa* (Bemis et al., 2002, medium light). For all other, species we used the calcite equation from Kim and O’Niel (1997), adapted to a quadratic form by Bemis et al., (1998) following the approach of Sime et al., (2005). To take into account the ecology of each species, theoretical $\delta^{18}\text{O}_c$ profiles were made for the season of maximum abundance (Table S4). Therefore spring and summer profiles were used for *T. sacculifer*, summer profiles used for *G. ruber*, and winter and annual average profiles was used for *N. dutertrei*. Annual average profiles were used for the other species.

For the two sites WP07-1 and A14, a different approach was necessary because $\delta^{18}\text{O}_c$ data is sparse. At these sites, and for our other sites, we utilized Mg/Ca-derived temperatures to estimate calcification depths (Table S6). $T_{\text{Mg/Ca}}$ was derived using species-specific Mg/Ca-temperature calibrations (Table S6) along with the Mg/Ca ratios determined in this study. Calcification depth was estimated by comparing $T_{\text{Mg/Ca}}$ to modern temperature profiles from the World Ocean atlas database 2013 (Boyer et al., 2013) in light of the ecology (seasonality of growth) of the species of interest. A caveat is that in certain cases $T_{\text{Mg/Ca}}$ may be partially biased by a carbonate ion effect or salinity effect (Russell et al., 2004; Elderfield et al., 2006; Ferguson et al., 2008; Arbuszewski et al., 2010; Martinez-Boti et al., 2011). These artifacts on $T_{\text{Mg/Ca}}$ may be significant at high-latitude sites such as CD107-a which is located in the North Atlantic Ocean.

Depth habitat

Planktonic foraminifera live in the upper 500 m of the water column. Their preferred depth habitat depends on their ecology, which in turn relies on the hydrographic conditions. For example, *G. ruber* is commonly found in the mixed layer (Fairbanks and Wiebe, 1980; Dekens et al., 2002; Farmer et al., 2007) during summer (Deuser et al., 1981) whereas *T. sacculifer* (n or ns) is present in the mixed layer until the mid-thermocline depth (Farmer et al., 2007) during spring and summer (Deuser et al., 1981, 1989). Specimens of *P. obliquiloculata* and *N. dutertrei* are found during winter (Deuser et al., 1989), in the mixed layer (~60m) for *P. obliquiloculata*, and at mid-thermocline depth for *N. dutertrei* (Farmer et al., 2007). Whereas, *O. universa* tends to record annual average conditions and is living within the mixed layer. Specimens of *G. menardii* calcify within the seasonal thermocline (Fairbanks et al., 1982, Farmer et al., 2007, Regenberg et al., 2009) even upper thermocline (Farmer et al., 2007) and records annual temperatures. And specimens of *G. tumida* are found at the lower thermocline or below the thermocline and record annual average conditions (Fairbanks and Wiebe, 1980; Farmer et al., 2007, Birch et al., 2013). Our calcification depth reconstructions are summarized in Table 3, also see Table S6 for comparison.

Atlantic Ocean

Farmer et al., (2007) determined the depth habitat for *O. universa* to be ranging from 0 to 60m (LL, Bemis et al., 1998). Our calculation, through $\delta^{18}\text{O}$ measurement, suggests a deeper habitat of around 70m (LL, Bemis et al., 1998), 80m (ML, Bemis et al., 2002). Whereas, the Mg/Ca method derived depth habitat calculation yields a depth habitat of 50 m. The lower habitat depth can also come from the different size fractions, as our size fraction is lower than Farmer’s. *O. universa* is thought to migrate to shallower depth along its ontogeny (Emiliani et al., 1954) younger individuals are thus living deeper but smaller individuals might also have a

deeper habitat as already suggested by Hönisch and Heming, (2004). Since most of the published studies have used the $\delta^{18}\text{O}$ -based depth calcification, we will preferentially adopt this method.

Indian Ocean

Calcification depths for the Indian Ocean cores have already been determined for majority of the species by Sime et al., (2005). Additionally, Birch et al., (2013) have reconstructed the depth habitat of multiple species from a core collected in the offshore region of Tanzania (Glow 3). In Indian Ocean specimens of *G. ruber* is found in the top 50m (Birch et al., 2013) and until 60 m (Sime et al., 2005), *T. sacculifer* is found in the surface mixed layer (SML) but also in the upper thermocline between 50-70 m for Birch et al., (2013) and between 60 to 80 m for Sime et al., (2005). Our results are consistent with these reported depth habitats. We calculate that specimens of *G. ruber*, *T. sacculifer* with and without sac are living in the top 80m; *O. universa* lives between 50 to 90 m (Sime et al., 2005, Birch et al., 2013). For *N. dutertrei* we calculate a depth habitat of 90m at site FC01a, calcification depths derived from both $\delta^{18}\text{O}$ and Mg/Ca methods agree with the 93 m estimate by Sime et al., (2005). At site FC02a the calculated calcification depth based on $\delta^{18}\text{O}$ method is 65 m, and, the Mg/Ca derived depth is 100m; however, Sime et al., (2005) proposed a calcification depth of 146 m. A deeper depth habitat than site FC01a seems to be in line with the weaker stratification of the water column at site FC02a. The depth habitat for *P. obliquiloculata*'s was determined to be 106–120m by Sime et al., (2005); however, our calculations predict a lower and narrower depth habitat of 60 – 70m. Calcification depth for *G. menardii* has been calculated to be 60 – 70m, which is consistent with an upper thermocline depth habitat. Specimens of *G. tumida* is commonly found at the bottom of the thermocline which is around 200-250m at our Indian Ocean sites, Birch et al., (2013) found this species ranging from 100 to 200 m but our $\delta^{18}\text{O}$ based habitat reconstruction suggests a shallower depth of 70m at both sites. It seems that the calcification derived Mg/Ca for *G. tumida* is more realistic than with our $\delta^{18}\text{O}_c$ reconstructions, the Mg/Ca based calculation predicts a depth habitat of 100 – 130 m.

Arabian Sea

In the Arabian Sea foraminifera are affected by changes in local hydrology caused by the Indian summer and winter monsoons. The specimens of different species collectively record a shallower habitat during SW monsoon (e.g., upwelling) and a deeper habitat during NE monsoon (Peeters and Brummer, 2002). Except for *N. dutertrei*, our two methods of calcification depth reconstruction closely agree with each other within their respective uncertainties. The depth habitat reconstructions for *G. ruber* and for *T. sacculifer* are consistent with species living in the shallow mixed layer (SML) at a depth of 30m for *G. ruber* and 40 m for *T. sacculifer*. Specimens of *O. universa* are calculated to live at 30m depth; *N. dutertrei* at site FC12-b (water depth 151m) is living around 40m and at 150m at site FC13-b (water depth 3200m), which is consistent with the hydrography at this site (Fig. 4). The depth habitat of *P. obliquiloculata* is calculated to be 50m at both sites. Specimens of *G. menardii* is found at depths of 60m, consistent with Peeters and Brummer, (2002) estimate of 50 – 130m.

Pacific Ocean

For Pacific Ocean samples the Mg/Ca derived calcification depths were used in absence of $\delta^{18}\text{O}_c$ values. The Sites WP07-01 and A14 are located in the Western Equatorial Pacific with Site WP07-01

characterized by a deep thermocline. At these sites *G. ruber* and *T. sacculifer* have deep depth habitat of around 100m for *G. ruber* (Elderfield and Ganssen, 2000) and around 125m for *T. sacculifer* (Rickaby et al., 2005). The depth habitat for specimens of *O. universa* was determined to be 75m depth at site WP07-01 and at 55m depth at site A14. We calculate that *P. obliquiloculata* is living at 125m deep. Rickaby et al., (2005) estimated the living depth of *N. dutertrei* at 165m in agreement with our calculated depths (~125m). Specimens of *G. menardii* were determined to live at 180m like *G. tumida* (Rickaby et al., 2005).

The data are not consistent with a dissolution effect to explain the low $\delta^{11}\text{B}$ *T. sacculifer* in the WEP

Documented dissolution effects have been attributed to the preferential dissolution of ontogenic calcite relative to the light $\delta^{11}\text{B}$ of gametogenic calcite (Ni et al., 2007; Seki et al., 2010; Henehan et al., 2016). *T. sacculifer* (w/o sacc) should be less impacted compared to the *T. sacculifer* (sacc). Hönisch and Hemming, (2004) and Ni et al., (2007) reported a dissolution effect at site 806 (close to our WP07-01 site) for *T. sacculifer* (sacc), however, in our data the $\delta^{11}\text{B}_{\text{carbonate}}$ for *T. sacculifer* (sacc) is not decreasing with water depth when *T. sacculifer* (w/o sacc) is which suggests that at these sites and at the same size-fraction no dissolution is observed (eg. different water depth). $\Delta^{11}\text{B}$ for *T. sacculifer* (w/o sacc) and for *G. ruber* shift to lighter with higher calcification depth, a trend that does not support a dissolution effect. The lethal temperature for *T. sacculifer* is 14°C, which at site WP07-01 corresponds to a $\delta^{11}\text{B}_{\text{borate}}$ of 17.5 ‰ which makes our low $\delta^{11}\text{B}_{\text{carbonate}}$ realistic. If no dissolution is observed, a deep depth habitat inducing a respiration-driven microenvironment might explain the low $\delta^{11}\text{B}$ of the measured carbonate.

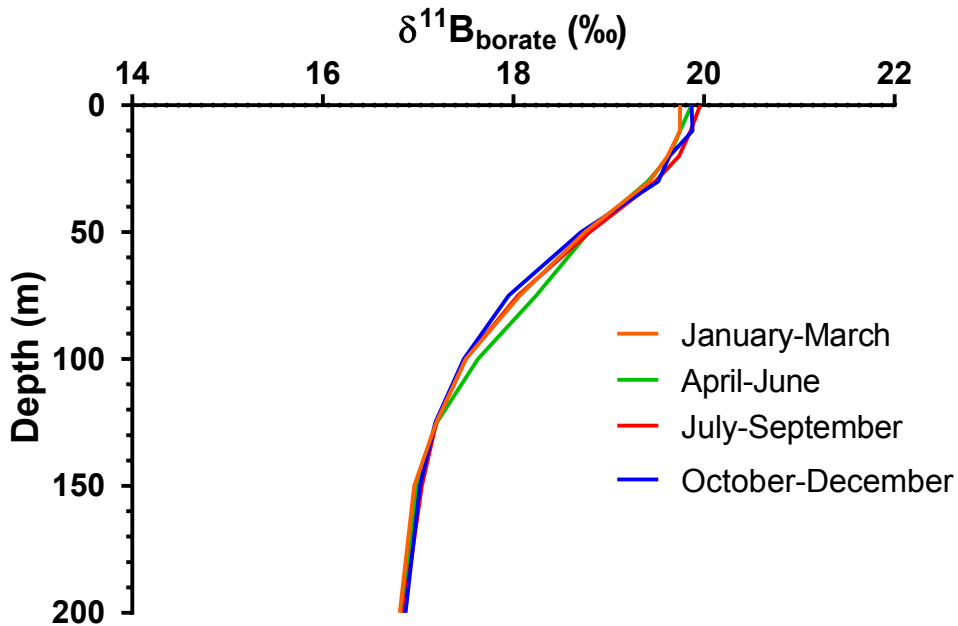
Microenvironment calculations

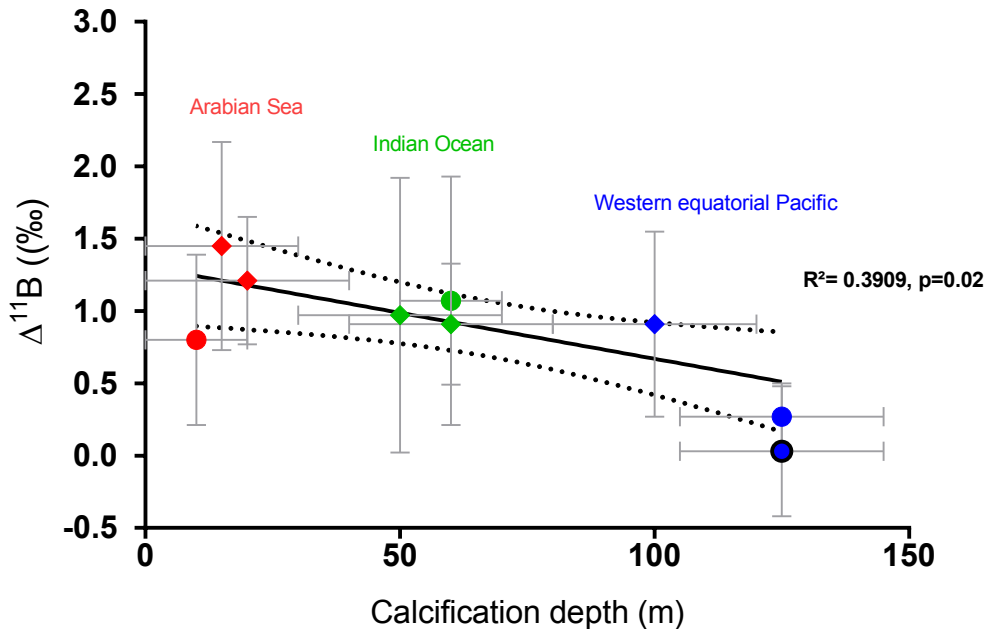
We observe a trend between $\Delta^{11}\text{B}$ (eg. $\Delta^{11}\text{B} = \delta^{11}\text{B}_{\text{carbonate}} - \delta^{11}\text{B}_{\text{borate}}$) with derived calcification depth (Fig. S2). In order to verify why the WEP $\delta^{11}\text{B}_{\text{carbonate}}$ of *T. sacculifer* (w/o sacc) is low and to test the hypothesis of the depth habitat we try to recalculate independently the theoretical water depth habitat based on culture results from Jorgensen et al., (1985) and our microenvironment pH results. A change of microenvironment pH for *T. sacculifer* will change the theoretical light intensity needed to reach this microenvironment pH. The compensation light intensity (E_c) for *T. sacculifer* has been calculated by Jorgensen et al., (1985) to be $\sim 30 \mu\text{Eistn.m}^{-2}.\text{s}^{-1}$, E_c corresponds to the energy where photosynthesis compensates respiration or where $\delta^{11}\text{B}_{\text{carbonate}}$ reaches the 1:1 theoretical line. We tested two microenvironment pH, $\Delta\text{pH}_1 = -0.04$ and $\Delta\text{pH}_2 = -0.06$ (Fig S3). We've recalculated the light energy needed to decrease the pH of ΔpH_1 and ΔpH_2 and apply these changes to the light penetration profile determined with an insolation E_0 in the WEP of $220 \text{ J.s}^{-1}.\text{m}^{-2}$ (Weare et al., 1981) and a light attenuation coefficient of 0.028 (Wang et al., 2008). A decrease of ΔpH_1 would lead to a decrease of $15 \mu\text{Eistn.m}^{-2}.\text{s}^{-1}$ and a decrease of ΔpH_2 would lead to a decrease of $24 \mu\text{Eistn.m}^{-2}.\text{s}^{-1}$ (Jorgensen et al., 1985). These results correspond in our case of a light penetration of 12% to reach E_c , 5% for a decrease of ΔpH_1 and 1% for a decrease of ΔpH_2 . This means that in the WEP if *T. sacculifer* calcifies below 75m where E_c is reached the $\delta^{11}\text{B}_{\text{carbonate}}$ is below the theoretical 1:1 line. *T. sacculifer* (w/o sacc) in the WEP is decreasing its pH of $\sim \Delta\text{pH}_1$ which would imply a calcification depth of 110m consistent with the reconstruction of Rickaby et al., (2005).

References

- Arbuszewski, J., DeMenocal, P., Kaplan, A. and Farmer, E. C.: On the fidelity of shell-derived $\delta^{18}\text{O}$ seawater estimates, *Earth Planet. Sci. Lett.*, 300, 185–196, 2010.
- Barker, S., Greaves, M. and Elderfield, H.: A study of cleaning procedures used for foraminiferal Mg/Ca paleothermometry, *Geochemistry, Geophys. Geosystems* 4, 1–20, 2003.
- Bemis, B. E., Spero, H. J. and Thunell, R. C.: Using species-specific paleotemperature equations with foraminifera: a case study in the Southern California Bight, *Mar. Micropaleontol.*, 46, 405–430, 2002.
- Bemis, B. E., Spero, H. J., Bijma, J. and Lea, D. W.: Reevaluation of the oxygen isotopic composition of planktonic foraminifera: Experimental results and revised paleotemperature equations, *Paleoceanography*, 13, 150–160, 1998.
- Birch, H., Coxall, H. K., Pearson, P. N., Kroon, D. and O'Regan, M.: Planktonic foraminifera stable isotopes and water column structure: Disentangling ecological signals, *Mar. Micropaleontol.*, 101, 127–145, 2013.
- Boyer, T.P., J. I. Antonov, O. K. Baranova, C. Coleman, H. E. Garcia, A. Grodsky, D. R. Johnson, R. A. Locarnini, A. V. Mishonov, T.D. O'Brien, C.R. Paver, J.R. Reagan, D. Seidov, I. V. Smolyar, and M. M. Zweng: World Ocean Database 2013, NOAA Atlas NESDIS 72, S. Levitus, Ed., A. Mishonov, Technical Ed.; Silver Spring, 2013
- Dekens, P. S., Lea, D. W., Pak, D. K. and Spero, H. J.: Core top calibration of Mg/Ca in tropical foraminifera: Refining paleotemperature estimation, *Geochemistry, Geophys. Geosystems*, 3, 1–29, 2002.
- Deuser, W.G., Ross, E.H., Hemleben, Ch., Spindler, M.: Seasonal changes in species composition, numbers, mass, size, and isotopic composition of planktonic foraminifera settling into the deep Sargasso Sea, *Palaeogeogr., Palaeoclimat., Palaeoecol.*, 33:103-127, 1981.
- Deuser, W. G. and Ross, E. H., Seasonally abundant planktonic foraminifera of the Sargasso Sea; succession, deep-water fluxes, isotopic compositions, and paleoceanographic implications, *J. Foraminifer. Res.*, 19, 268–293, 1989.
- Duplessy, J., Labeyrie, L., Juilletleclerc, A., Maitre, F., Duprat, J. and Sarnthein, M., Surface salinity reconstruction of the north-atlantic ocean during the last glacial maximum, *Oceanol. Acta*, 14, 311–324, 1991.
- Elderfield, H., Yu, J., Anand, P., Kiefer, T. and Nyland, B.: Calibrations for benthic foraminiferal Mg/Ca paleothermometry and the carbonate ion hypothesis, *Earth Planet. Sci. Lett.*, 250, 633–649, 2006.
- Farmer, E. C., Kaplan, A., de Menocal, P. B. and Lynch-Stieglitz, J.: Corroborating ecological depth preferences of planktonic foraminifera in the tropical Atlantic with the stable oxygen isotope ratios of core top specimens, *Paleoceanography*, 22, 1–14, 2007.
- Fairbanks, R. G., Sverdrlove, M., Free, R., Wiebe, P. H. and Bé, A. W. H.: Vertical distribution and isotopic fractionation of living planktonic foraminifera from the Panama Basin, *Nature*, 298, 841–844, 1982.
- Fairbanks, R. G. and Wiebe, P. H., Foraminifera and Chlorophyll Maximum: Vertical Distribution, Seasonal Succession, and Paleoceanographic Significance, *Science*, 209, 1524–1526, 1980.
- Ferguson, J. E., Henderson, G. M., Kucera, M. and Rickaby, R. E. M.: Systematic change of foraminiferal Mg/Ca ratios across a strong salinity gradient, *Earth Planet. Sci. Lett.*, 265, 153–166, 2008.
- Henehan, M. J., Foster, G. L., Bostock, H. C., Greenop, R., Marshall, B. J. and Wilson, P. A.: A new boron isotope-pH calibration for *Orbulina universa*, with implications for understanding and accounting for 'vital effects.', *Earth Planet. Sci. Lett.*, 454, 282–292, 2016.

- Hönisch, B. and Hemming, N. G.: Ground-truthing the boron isotope-paleo-pH proxy in planktonic foraminifera shells: Partial dissolution and shell size effects, *Paleoceanography*, 19, 1–13, 2004.
- Jørgensen, B. B., Erez, J., Revsbech, P. and Cohen, Y.: Symbiotic photosynthesis in a planktonic foraminiferan, *Globigerinoides sacculifer* (Brady), studied with microelectrodes, *Limnol. Oceanogr.* 30, 1253–1267, 1985.
- Kim, S.-T. and O’Neil, J. R.: Equilibrium and nonequilibrium oxygen isotope effects in synthetic carbonates, *Geochim. Cosmochim. Acta*, 61, 3461–3475, 1997.
- Martínez-Botí, M. A., Mortyn, P. G., Schmidt, D. N., Vance, D. and Field, D. B.: Mg/Ca in foraminifera from plankton tows: Evaluation of proxy controls and comparison with core tops, *Earth Planet. Sci. Lett.*, 307, 113–125, 2011.
- Misra, S., Greaves, M., Owen, R., Kerr, J., Elmore, A. C. and Elderfield, H.: Determination of B/Ca of natural carbonates by HR-ICP-MS, *Geochemistry, Geophys. Geosystems*, 15, 1617–1628, 2014.
- Mulitza, S., Boltovskoy, D., Donner, B., Meggers, H., Paul, A. and Wefer, G.: Temperature:δ18O relationships of planktonic foraminifera collected from surface waters, *Palaeogeogr. Palaeoclimatol. Palaeoecol.* 202, 143–152, 2003.
- Ni, Y., Foster, G. L., Bailey, T., Elliott, T., Schmidt, D. N., Pearson, P., Haley, B. and Coath, C.: A core top assessment of proxies for the ocean carbonate system in surface-dwelling foraminifers, *Paleoceanography*, 22, 2007.
- Peeters, F. J. C. and Brummer, G.-J. a.: The seasonal and vertical distribution of living planktic foraminifera in the NW Arabian Sea, *Geol. Soc. London, Spec. Publ.*, 195, 463–497, 2002.
- Rostek, F., Ruhland, G., Bassinot, F. C., Muller, P. J., Labeyrie, L. D., Lancelot, Y. and Bard, E.: Reconstructing Sea-Surface Temperature and Salinity Using δ18O and Alkenone Records, *Nature*, 364, 319–321, 1993.
- Russell, A. D., Hönisch, B., Spero, H. J. and Lea, D. W.: Effects of seawater carbonate ion concentration and temperature on shell U, Mg, and Sr in cultured planktonic foraminifera, *Geochim. Cosmochim. Acta*, 68, 4347–4361, 2004.
- Seki, O., Foster, G. L., Schmidt, D. N., Mackensen, A., Kawamura, K. and Pancost, R. D.: Alkenone and boron-based Pliocene pCO₂ records, *Earth Planet. Sci. Lett.*, 292, 201–211, 2010.
- Sime, N. G., De La Rocha, C. L. and Galy, A.: Negligible temperature dependence of calcium isotope fractionation in 12 species of planktonic foraminifera, *Earth Planet. Sci. Lett.*, 232, 51–66, 2005.
- Yu, J., Day, J., Greaves, M. and Elderfield, H.: Determination of multiple element/calcium ratios in foraminiferal calcite by quadrupole ICP-MS, *Geochemistry, Geophys. Geosystems* 6, 2005.
- Rickaby, R. E. M. and Halloran, P.: Cool La Nina During the Warmth of the Pliocene?, *Science*, 307, 1948–1952, 2005.
- Wang, G., Cao, W., Yang, D. and Xu, D. Variation in downwelling diffuse attenuation coefficient in the northern South China Sea, *Chinese J. Oceanol. Limnol.*, 26, 323–333, 2008.
- Weare, B. C., Strub, P. T. and Samuel, M. D.: Annual Mean Surface Heat Fluxes in the Tropical Pacific Ocean, *J. Phys. Oceanogr.*, 11, 705–717, 1981.





◆ *G. ruber* (Arabian Sea)

● *T. sacculifer* (w/sacc) (Arabian Sea)

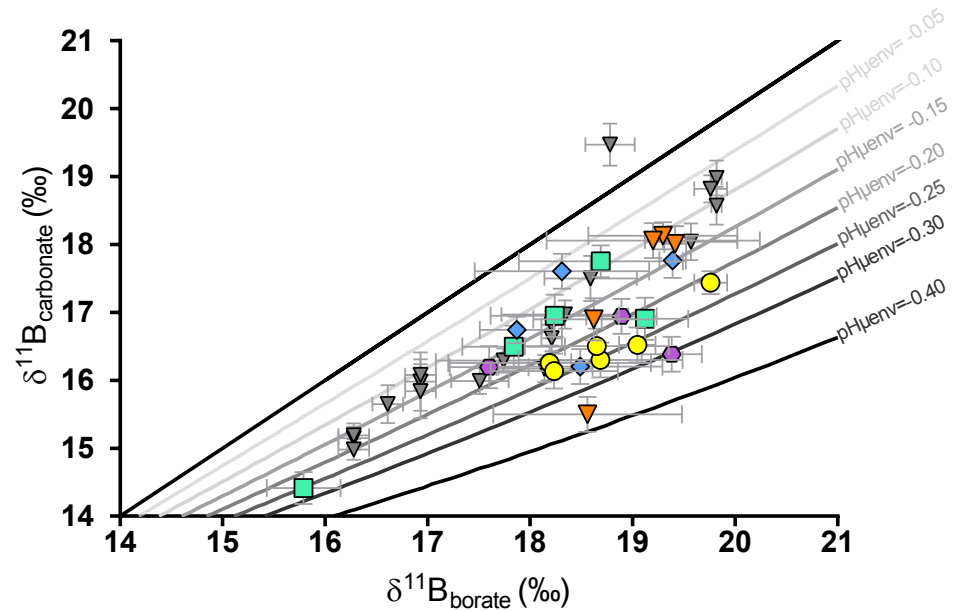
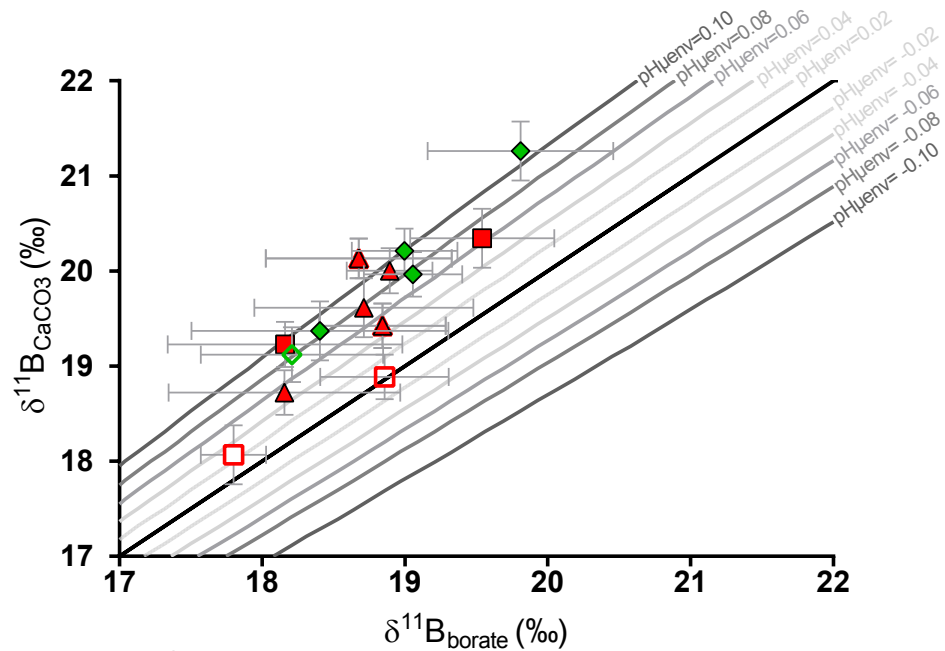
◆ *G. ruber* (Indian Ocean)

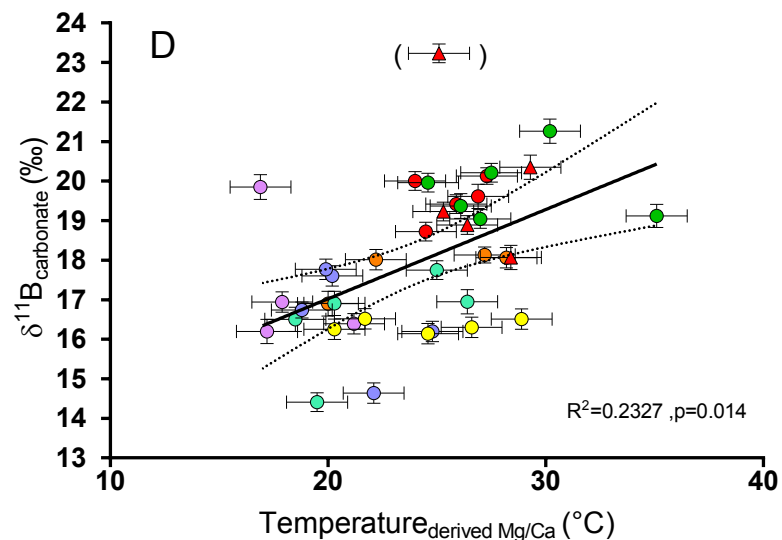
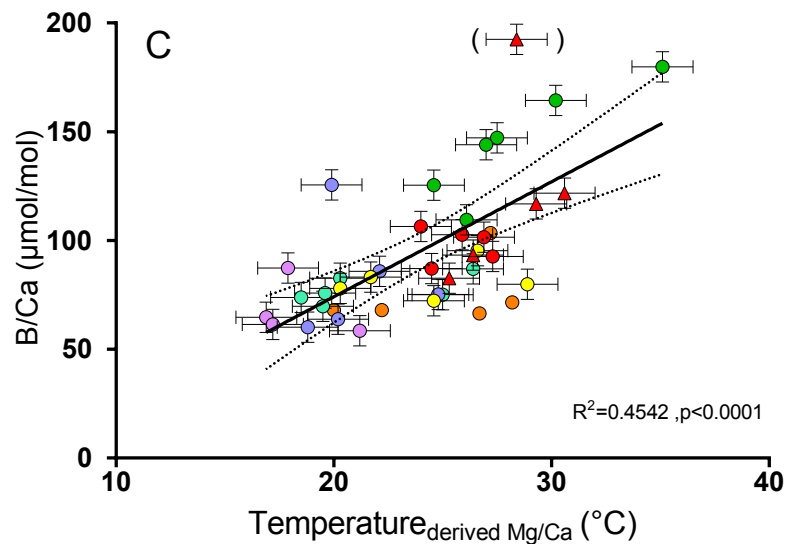
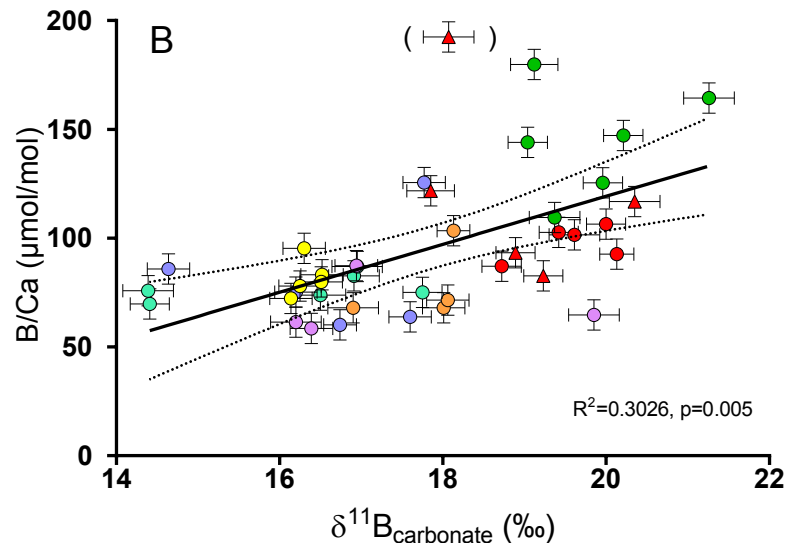
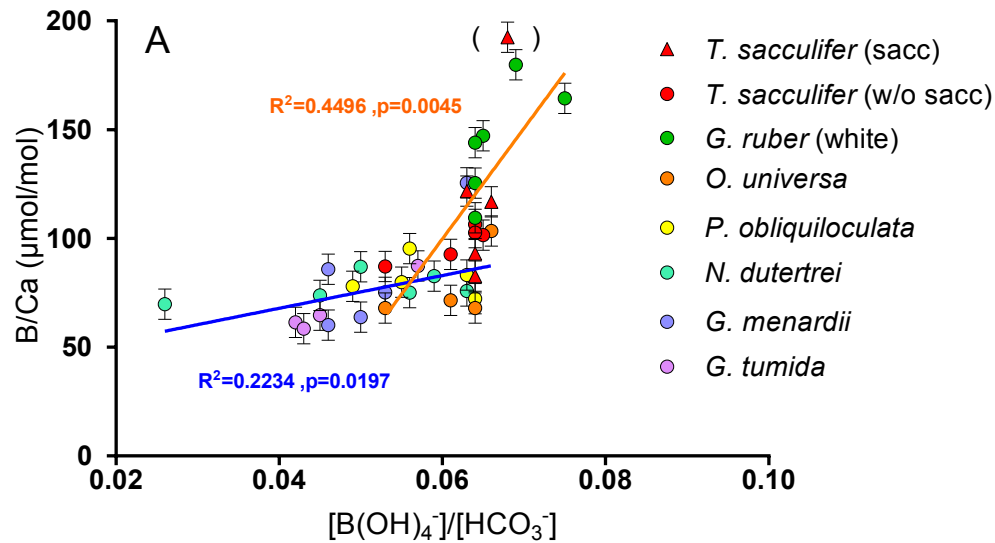
● *T. sacculifer* (w/o sacc) (Indian Ocean)

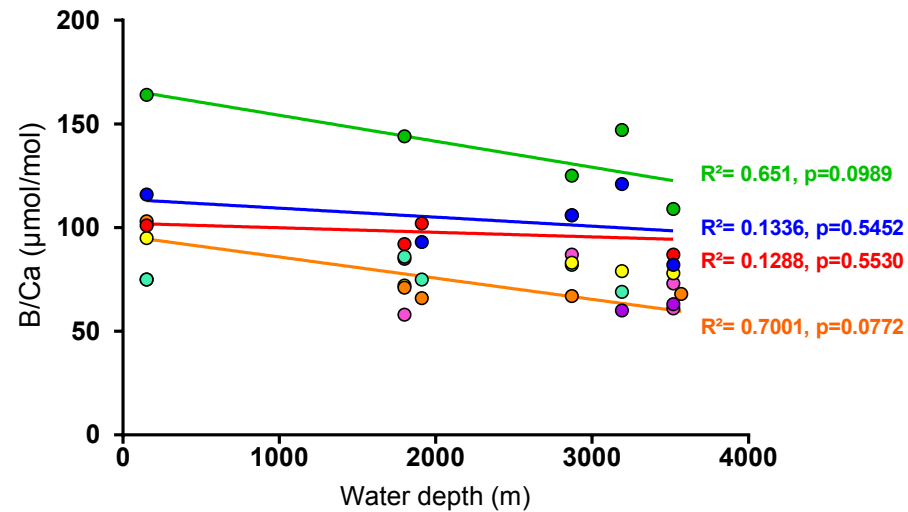
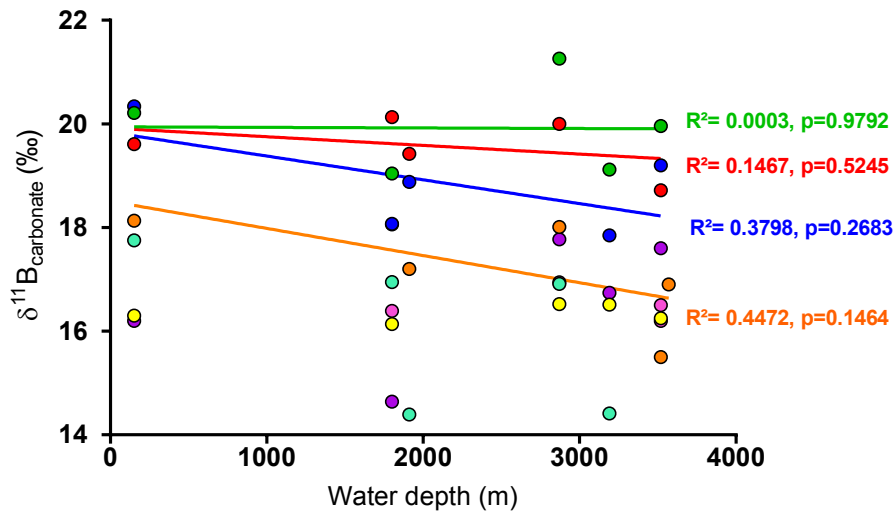
◆ *G. ruber* (WEP)

● *T. sacculifer* (w/o sacc) (WEP)

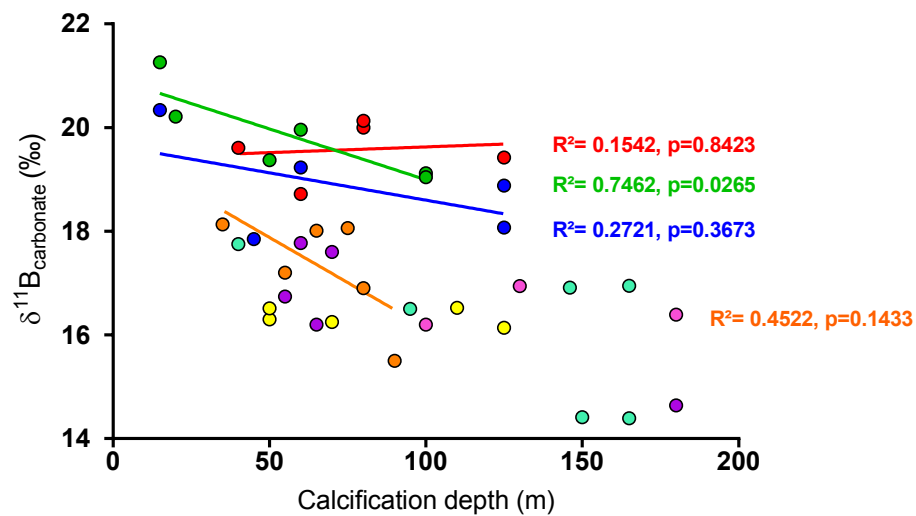
— Linear reg. All species







- *G. ruber*
- *T. sacculifer* (w/o sacc)
- *T. sacculifer* (sacc)
- *O. universa*
- *P. obliquiloculata*
- *N. dutertrei*
- *G. menardii*
- *G. tumida*



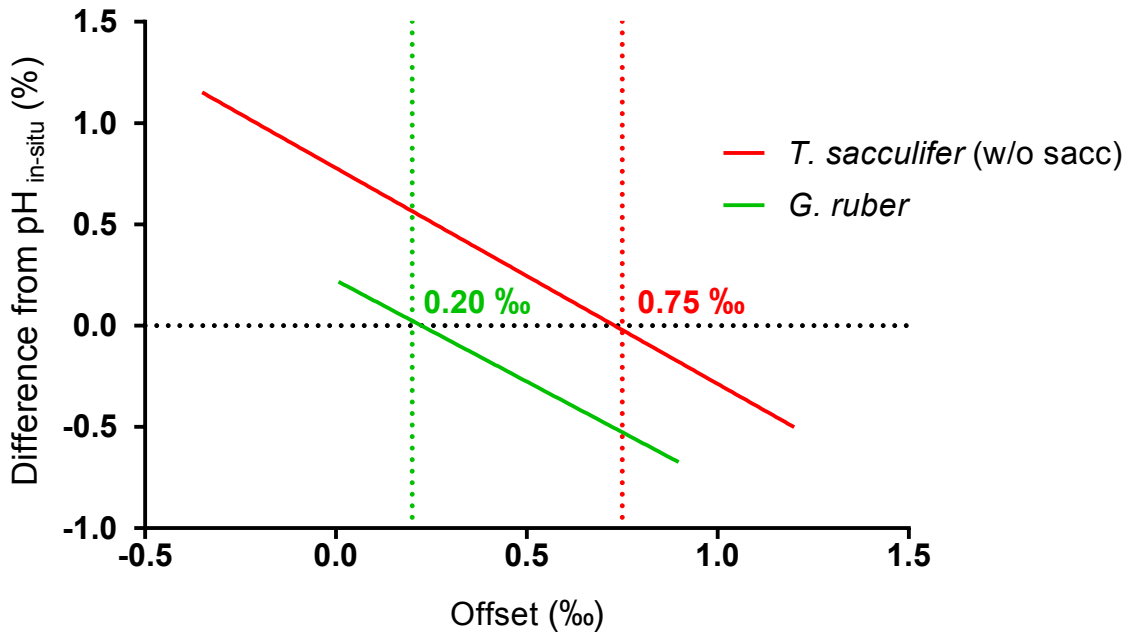


Table S1

Elemental ratios	Li/Ca μmol/mol	B/Ca μmol/mol	Mg/Ca mmol/mol	Al/Ca mmol/mol	Sr/Ca mmol/mol	Cd/Ca μmol/mol	Ba/Ca μmol/mol	U/Ca nmol/mol	Mn/Ca μmol/mol	Fe/Ca mmol/mol
Standard solution 0	0.8	9	0.10	0.131	0.00	0.03	0.6	31	1	0.01
Standard solution 1	2.3	38	0.31	0.112	0.49	0.05	1.9	38	12	0.02
Standard solution 3	6.8	108	1.31	0.177	1.06	0.13	3.0	53	39	0.04
Standard solution 5	14.6	216	3.17	0.223	1.57	0.23	5.1	62	129	0.08
Standard solution 6	19.0	278	5.23	0.352	1.97	0.28	5.5	74	196	0.11
Standard solution 8	25.0	281	6.07	0.602	2.99	0.50	20.1	390	501	0.50
Standard solution 9		408			4.89					
Standard solution 10		519			8.01					
Standard solution 11		607			9.93					

Table S2

Standard	$\delta^{11}\text{B}_1$ (‰)	$2\text{SD}_{\text{AEI21}}$	n_{AEI21}	$\delta^{11}\text{B}_2$ (‰)	$2\text{SD}_{\text{AEI21}}$	n_{AEI21}	Reference
NEP1	25.21	0.25	11	25.22	0.25	11	This study
NEP2	25.00	0.30	12				This study
NEP3	24.70	0.30	12				This study
NEP4	25.40	0.21	11				This study
NEP5	25.32	0.21	11	25.33	0.21	11	This study
NEP6	25.22	0.21	11				This study
NEP7	25.26	0.26	15				This study
NEP8	25.39	0.26	15				This study
NEP9	26.15	0.26	15				This study
NEP10	25.97	0.26	15				This study
NEP11	26.09	0.26	15	26.09	0.26	15	This study
NEP12	26.22	0.26	15	26.29	0.26	15	This study
NEP13	26.19	0.26	15	26.21	0.26	15	This study
NEP14	26.12	0.26	15	26.13	0.26	15	This study
NEP15	26.00	0.26	15				This study
NEP16	26.04	0.26	15				This study
NEP17	26.02	0.29	12				This study
NEP18	25.86	0.29	12	25.86	0.26	14	This study
NEP19	25.78	0.26	14				This study
NEP20	25.42	0.15	3	25.32	0.15	3	This study
NEP21	25.54	0.22	6	26.16	0.22	6	This study
NEP22	26.42	0.22	6				This study
JCP-1-1	24.07	0.10					This study
JCP-1-2	24.17	0.11		24.17	0.10		This study
JCP-1-3	24.01	0.11					This study
JCP-1-4	23.92	0.26					This study
JCP-1-5	24.03	0.26		24.05	0.39		This study
JCP-1-6	24.18	0.36		24.16	0.36		This study
Standard	Average $\delta^{11}\text{B}$	2SD	n	Reference			
NEP	25.70	0.93	22	This study			
NEP	26.20	0.88	27	Holcomb et al., 2015			
NEP	25.80	0.89	6	Sutton et al., 2018			
JCP-1	24.06	0.20	6	This study			
JCP-1	24.37	0.32	57	Holcomb et al., 2015			
JCP-1	24.42	0.28	7	Sutton et al., 2018			

Table S4

Specie	Seasonality
<i>T. sacculifer (sacc)</i>	Spring
<i>T. sacculifer (w/o sacc)</i>	Spring
<i>G. ruber (white)</i>	Summer
<i>N. dutertrei</i>	Winter
<i>G. tumida</i>	Annual average
<i>G. menardii</i>	Annual average
<i>O. universa</i>	Annual average
<i>P. obliquiloculata</i>	Winter

Table S5

Species	B	A	Reference
<i>T. sacculifer (sacc)</i>	0.377	0.090	Anand et al., 2003
<i>T. sacculifer (w/o sacc)</i>	0.347	0.090	Anand et al., 2003
<i>G. ruber (white)</i>	0.300	0.089	Dekens et al., 2002
<i>N. dutertrei</i>	0.600	0.008	Dekens et al., 2002
<i>G. tumida</i>	0.380	0.090	Anand et al., 2003
<i>G. menardii</i>	0.360	0.091	Regenberg et al., 2009
<i>O. universa</i>	0.595	0.090	Anand et al., 2003
<i>P. obliquiloculata</i>	0.328	0.090	Anand et al., 2003

Species	A	B	C	dw correction	Condition	Reference	Equation
<i>O. universa</i>	16.500	4.800		-0.27	LL	Bemis et al., 1998	$T=A-B*(\delta^{18}O_c-\delta^{18}O_w)$
<i>O. universa</i>	15.700	4.460	0.35	-0.27	ML	Bemis et al., 2002	$T=A-B*(\delta^{18}O_c-\delta^{18}O_w)+C*(\delta^{18}O_c-\delta^{18}O_w)^2$
<i>O. universa</i>	14.900	4.800		-0.27	HL	Bemis et al., 1998	$T=A-B*(\delta^{18}O_c-\delta^{18}O_w)$
<i>T. sacculifer</i>	14.910	4.350		-0.27		Mulitza et al., 2003	$T=A-B*(\delta^{18}O_c-\delta^{18}O_w)$
<i>G. ruber</i>	14.200	4.440		-0.27		Mulitza et al., 2003	$T=A-B*(\delta^{18}O_c-\delta^{18}O_w)$
All	16.900	4.380	0.1	-0.2		Shackleton et al., 1974	$T=A-B*(\delta^{18}O_c-\delta^{18}O_w)+C*(\delta^{18}O_c-\delta^{18}O_w)^2$
All	17.000	4.520	0.03	-0.22		Erez and Luz, 1983	$T=A-B*(\delta^{18}O_c-\delta^{18}O_w)+C*(\delta^{18}O_c-\delta^{18}O_w)^2$
All	16.100	4.640	0.09	-0.27		Kim and O'Neil 1997	$T=A-B*(\delta^{18}O_c-\delta^{18}O_w)+C*(\delta^{18}O_c-\delta^{18}O_w)^3$

Table S6

Core	Species	CD ₁	CD ₂	CD ₃	Reference
FC-01a	<i>G. ruber</i> (white ss)	83 ± 20	30 ± 10	50 ± 20	Sime thesis 2006
FC-02a	<i>G. ruber</i> (white ss)	56 ± 10	15 ± 10	60 ± 20	Sime thesis 2006
FC-12b	<i>G. ruber</i> (white ss)	Surface ± 10	0-30	60 ± 10	Peeters and Brumer, 2012 (non upwelling station Arabian sea)
FC-13a	<i>G. ruber</i> (white ss)	Surface ± 10	20 ± 20	60 ± 10	Peeters and Brumer, 2012 (non upwelling station Arabian sea)
WP7-01	<i>G. ruber</i> (white ss)			100±20	Elderfield and Ganssen, 2000
A14	<i>G. ruber</i> (white ss)		60 ± 10	100±20	Elderfield and Ganssen, 2000
FC-01a	<i>T. sacculifer</i> (sacc)	48 ± 10	50 ± 10	60 ± 10	Sime et al., 2005
FC-02a	<i>T. sacculifer</i> (sacc)	7 ± 10	30 ± 10	80 ± 20	Sime et al., 2006
FC-12b	<i>T. sacculifer</i> (sacc)	15 ± 10	40 ± 10		
WP7-01	<i>T. sacculifer</i> (sacc)		80 ± 20	125 ± 15	Rickaby et al., 2005
A14	<i>T. sacculifer</i> (sacc)		60 ± 10	125 ± 15	
FC-01a	<i>T. sacculifer</i> (w/o sacc)	88 ± 20	50 ± 10	60 ± 10	Sime thesis 2006 (Wind22-b)
FC-02a	<i>T. sacculifer</i> (w/o sacc)	32 ± 10	10 ± 10	80 ± 20	Sime thesis 2006
FC-12b	<i>T. sacculifer</i> (w/o sacc)	0-15 ± 10	30 ± 10	45 ± 20	Peeters and Brumer, 2012 (non upwelling station Arabian sea)
WP7-01	<i>T. sacculifer</i> (w/o sacc)		80 ± 20	125 ± 15	Rickaby et al., 2005
A14	<i>T. sacculifer</i> (w/o sacc)		60 ± 10	125 ± 15	Rickaby et al., 2005
CD107a	<i>O. universa</i>	80 ± 20	50 ± 20	0-50	Farmer et al., 2007
FC-01a	<i>O. universa</i>	45 ± 10	60 ± 10	90 ± 20	Sime et al., 2005
FC-02a	<i>O. universa</i>	127 ± 20	45 ± 15	65 ± 10	Birshe et al., 2013
FC-12b	<i>O. universa</i>	35 ± 10	30 ± 20		
WP7-01	<i>O. universa</i>		75 ± 25		
A14	<i>O. universa</i>		55 ± 15		
FC-01a	<i>P. obliquiloculata</i>	70 ± 20	75 ± 15	106 ± 20	Sime et al., 2005
FC-02a	<i>P. obliquiloculata</i>	226 ± 20	60 ± 10		
FC-12b	<i>P. obliquiloculata</i>	40 ± 10	50 ± 10		
FC-13a	<i>P. obliquiloculata</i>	65 ± 10	50 ± 10		
WP7-01	<i>P. obliquiloculata</i>		125 ± 25		
FC-01a	<i>N. dutertrei</i>	95 ± 20	90 ± 20	93 ± 20	Sime et al., 2005
FC-02a	<i>N. dutertrei</i>	65 ± 10	100 ± 20	146 ± 20	Sime et al., 2005
FC-12b	<i>N. dutertrei</i>	40 ± 10	50 ± 10		
FC-13a	<i>N. dutertrei</i>	45 ± 10	150 ± 20		
WP7-01	<i>N. dutertrei</i>		125 ± 25	165	Rickaby et al., 2005
A14	<i>N. dutertrei</i>		110 ± 20	165	Rickaby et al., 2005
FC-01a	<i>G. menardii</i>	135 ± 20	70 ± 20		
FC-02a	<i>G. menardii</i>	60 ± 10	60 ± 10		
FC-12b	<i>G. menardii</i>	65 ± 10	55 ± 15	60 ± 10	Peeters and Brumer, 2012 (non upwelling station Arabian sea)
FC-13a	<i>G. menardii</i>	55 ± 10	70 ± 10	60 ± 10	Peeters and Brumer, 2012 (non upwelling station Arabian sea)
WP7-01	<i>G. menardii</i>		180 ± 20		
FC-01a	<i>G. tumida</i>	70 ± 20	100 ± 10	160 ± 20	Birshe et al., 2013
FC-02a	<i>G. tumida</i>	70 ± 20	130 ± 20	160 ± 20	Birshe et al., 2013
WP7-01	<i>G. tumida</i>		180 ± 20	210 - 240	Rickaby et al., 2005

CD₁: Depth habitat estimated from δ¹⁸O_c

CD₂: Depth habitat estimated from Mg/Ca derived temperature

CD₃: Depth habitat from literature

Table S7

Core	Species	Depth habitat (m)	PRE INDUSTRIAL IN-SITU PARAMETERS																CALCULATED PARAMETERS							
			Temperature (°C)	2sd* Salinity	2sd* pH (pre-ind)	2sd* pCO ₂	2sd* HCO ₃ ⁻	2sd* CO ₃ ²⁻	2sd* DIC	2sd* ALK	2sd* δ ¹¹ B _{borate}	2sd*	T _{Mg/Ca}	2sd	pH _{d11B}	2sd**	pCO ₂	2sd***								
Atlantic Ocean																										
CD107a	<i>O. universa</i>	80 ± 20	12.0	0.3	35.6	0.01	8.19	0.03	274	21	1856	29	192	12	2059	18	2333	1	17.86	0.31	20.0	1.4	8.19	0.06	285	39
Indian Ocean																										
FC-01a	<i>G. ruber (white ss)</i>	50 ± 20	23.4	5.9	35.0	0.4	8.10	0.04	338	41	1743	138	226	48	1979	93	2299	22	18.40	0.90	26.1	1.4	8.07	0.05	387	29
FC-01a	<i>T. sacculifer (sacc)</i>	60 ± 10	21.9	5.7	35.1	0.3	8.09	0.03	346	38	1773	126	215	45	1998	84	2303	18	18.15	0.81	24.5	1.4	8.06	0.04	400	79
FC-01a	<i>T. sacculifer (w/o sacc)</i>	60 ± 10	21.9	5.7	35.1	0.3	8.09	0.03	346	38	1773	126	215	45	1998	84	2303	18	18.16	0.82	25.3	1.4	8.10	0.04	357	49
FC-01a	<i>O. universa</i>	90 ± 20	18.2	4.0	35.2	0.0	8.07	0.04	374	43	1856	94	184	35	2053	62	2311	9	17.42	0.61			7.98	0.06	499	63
FC-01a	<i>P. obliquiloculata</i>	70 ± 20	20.5	4.6	35.2	0.1	8.09	0.03	353	32	1802	99	204	36	2018	65	2306	11	17.91	0.66	20.3	1.4	8.10	0.08	356	48
FC-01a	<i>G. menardii</i>	70 ± 20	20.5	4.6	35.2	0.1	8.09	0.03	353	32	1802	99	204	36	2018	65	2306	11	17.93	0.68	20.2	1.4	8.16	0.05	304	43
FC-01a	<i>N. dutertrei</i>	95 ± 20	17.7	4.0	35.1	0.0	8.06	0.04	380	43	1868	94	180	35	2061	62	2313	9	17.26	0.62	18.5	1.4	8.09	0.06	373	49
FC-01a	<i>G. tumida</i>	100 ± 20	17.1	1.6	35.1	0.0	8.06	0.02	386	22	1881	41	175	15	2070	27	2314	3	17.21	0.27	17.2	1.4	8.06	0.07	400	52
FC-02a	<i>G. ruber (white ss)</i>	60 ± 20	20.4	2.4	35.5	0.0	8.19	0.01	268	10	1724	26	246	10	1979	17	2332	2	19.06	0.34	24.6	1.4	8.13	0.04	332	26
FC-02a	<i>T. sacculifer (sacc)</i>	80 ± 20	19.3	1.9	35.6	0.1	8.19	0.01	268	7	1741	38	240	15	1989	24	2333	3	18.89	0.30	24.0	1.4	8.18	0.03	286	57
FC-02a	<i>T. sacculifer (w/o sacc)</i>	80 ± 20	19.3	1.9	35.6	0.1	8.19	0.01	268	7	1741	38	240	15	1989	24	2333	3	18.90	0.30	25.1	1.4				
FC-02a	<i>O. universa</i>	65 ± 10	20.1	1.1	35.5	0.0	8.19	0.00	268	2	1728	15	245	6	1981	9	2332	1	19.00	0.17	22.2	1.4	8.18	0.04	287	42
FC-02a	<i>P. obliquiloculata</i>	110 ± 20	18.3	0.5	35.6	0.0	8.18	0.01	277	8	1769	17	228	7	2007	10	2334	1	18.64	0.14	21.7	1.4	8.16	0.08	302	43
FC-02a	<i>G. menardii</i>	60 ± 10	20.4	1.9	35.5	0.0	8.19	0.01	268	10	1724	19	246	7	1979	12	2332	2	19.05	0.30	19.9	1.4	8.17	0.05	293	42
FC-02a	<i>N. dutertrei</i>	146 ± 20	17.5	1.0	35.6	0.1	8.16	0.02	292	14	1798	31	216	13	2024	18	2333	2	18.33	0.27	20.3	1.4	8.12	0.06	339	46
FC-02a	<i>G. tumida</i>	130 ± 20	17.8	0.8	35.6	0.0	8.17	0.02	284	17	1784	32	222	14	2015	19	2334	1	18.47	0.25	17.9	1.4	8.12	0.05	339	46
Arabian Sea																										
FC-12b	<i>G. ruber (white ss)</i>	0-30	25.9	0.3	36.6	0.1	8.18	0.05	271	39	1655	53	292	23	1954	31	2374	8	19.81	0.65	30.2	1.4	8.15	0.04	305	28
FC-12b	<i>T. sacculifer (sacc)</i>	40 ± 10	25.3	0.6	36.5	0.0	8.10	0.06	350	64	1756	75	249	31	2015	46	2369	2	18.71	0.77	26.9	1.4	8.08	0.05	379	55
FC-12b	<i>T. sacculifer (w/o sacc)</i>	15 ± 10	25.9	0.0	36.5	0.1	8.16	0.04	290	34	1681	45	281	19	1970	28	2374	8	19.54	0.50	29.3	1.4	8.13	0.04	332	50
FC-12b	<i>O. universa</i>	35 ± 10	25.5	0.6	36.5	0.0	8.11	0.06	334	56	1738	68	257	28	2004	41	2369	1	18.90	0.69	27.2	1.4	8.13	0.03	336	50
FC-12b	<i>P. obliquiloculata</i>	50 ± 10	25.0	0.9	36.5	0.1	8.06	0.06	382	69	1794	75	233	32	2038	45	2368	3	18.24	0.67	26.6	1.4	8.05	0.08	415	58
FC-12b	<i>G. menardii</i>	65 ± 10	24.1	1.1	36.4	0.1	8.02	0.06	438	72	1850	75	209	32	2072	45	2365	4	17.69	0.62	24.8	1.4	7.97	0.06	514	68
FC-12b	<i>N. dutertrei</i>	40 ± 10	25.3	0.6	36.5	0.0	8.10	0.06	350	64	1756	75	249	31	2015	46	2369	2	18.75	0.71	25.0	1.4	8.11	0.04	350	52
FC-13a	<i>G. ruber (white ss)</i>	20 ± 20	27.1	1.1	36.7	0.1	8.10	0.03	343	27	1724	43	263	17	1996	26	2371	2	19.00	0.37	27.5	1.4	8.11	0.04	351	29
FC-13a	<i>T. sacculifer (w/o sacc)</i>	45 ± 20	25.7	0.7	36.6	0.0	8.07	0.03	380	34	1782	38	239	16	2032	23	2371	2	18.86	0.45	30.6	1.4				
FC-13a	<i>P. obliquiloculata</i>	50 ± 10	25.4	1.2	36.6	0.1	8.06	0.05	391	59	1797	66	233	29	2041	40	2370	4	18.31	0.57	28.9	1.4	8.08	0.08	385	55
FC-13a	<i>G. menardii</i>	55 ± 10	25.1	1.3	36.6	0.1	8.04	0.05	409	65	1815	69	225	30	2052	41	2369	5	18.04	0.56	18.8	1.4	7.98	0.04	503	68
FC-13a	<i>N. dutertrei</i>	150 ± 20	19.4	2.3	36.0	0.1	7.80	0.03	766	45	2056	37	118	15	2199	25	2348	1	15.37	0.27	19.5	1.4	7.79	0.08	811	101
Pacific Ocean																										
WP07-a	<i>G. ruber (white ss)</i>	100±20	26.1	2.4	35.2	0.4	8.05	0.05	387	51	1753	81	224	31	1988	52	2305	7	18.21	0.64	27.0	1.4	8.07	0.05	381	29
WP07-a	<i>T. sacculifer (sacc)</i>	80 ± 20	27.4	2.2	35.0	0.5	8.08	0.05	357	56	1708	89	242	33	1960	58	2303	10	18.68	0.65	27.3	1.4	8.10	0.03	350	52
WP07-a	<i>T. sacculifer (w/o sacc)</i>	125 ± 20	24.7	1.8	35.4	0.2	8.03	0.00	413	30	1797	31	209	9	2017	23	2311	10	17.80	0.23	28.4	1.4	8.03	0.05	427	58
WP07-a	<i>O. universa</i>	75 ± 25	27.7	2.6	34.9	0.6	8.09	0.07	349	68	1696	110	247	39	1953	73	2303	15	18.78	0.83	28.2	1.4	8.10	0.04	352	52
WP07-a	<i>P. obliquiloculata</i>	125 ± 25	24.7	3.6	35.4	0.4	8.03	0.02	413	30	1797	80	209	26	2017	56	2311	18	17.82	0.48	24.6	1.4	8.03	0.08	430	58
WP07-a	<i>N. dutertrei</i>	165 ± 20	20.6	3.8	35.5	0.2	8.03	0.01	408	10	1855	44	189	18	2057	26	2322	0	17.34	0.45	26.4	1.4	8.09	0.06	369	50
WP07-a	<i>G. tumida</i>	180 ± 20	18.7	5.0	35.4	0.2	8.04	0.01	403	13	1877	58	180	24	2070	35	2322	0	17.23	0.56	21.2	1.4	8.05	0.06	406	53

* uncertainties calculated using Henehan's 2016 R code

** propagated uncertainty on pH including d11B, temperature, salinity uncertainties

*** propagated uncertainty on pCO₂ including d11B, temperature, salinity, Alk uncertainties